# Pursuing the Precision Study for Color Glass Condensate in Forward Hadron Productions

Yu Shi,[1,2,*] Lei Wang,[2,†] Shu-Yi Wei,[1,3,‡] and Bo-Wen Xiao[4,§]

[1]*Key Laboratory of Particle Physics and Particle Irradiation (MOE), Institute of Frontier and Interdisciplinary Science, Shandong University, Qingdao, Shandong 266237, China*

[2]*Key Laboratory of Quark and Lepton Physics (MOE) and Institute of Particle Physics, Central China Normal University, Wuhan 430079, China*

[3]*European Centre for Theoretical Studies in Nuclear Physics and Related Areas (ECT*) and Fondazione Bruno Kessler, Strada delle Tabarelle 286, I-38123 Villazzano (TN), Italy*

[4]*School of Science and Engineering, The Chinese University of Hong Kong, Shenzhen 518172, China*

(Received 5 January 2022; revised 27 March 2022; accepted 5 May 2022; published 20 May 2022)

With the tremendous accomplishments of RHIC and the LHC experiments and the advent of the future electron-ion collider on the horizon, the quest for compelling evidence of the color glass condensate (CGC) has become one of the most aspiring goals in the high energy quantum chromodynamics research. Pursuing this question requires developing the precision test of the CGC formalism. By systematically implementing the threshold resummation, we significantly improve the stability of the next-to-leading-order calculation in CGC for forward rapidity hadron productions in $pp$ and $pA$ collisions, especially in the high $p_T$ region, and obtain reliable descriptions of all existing data measured at RHIC and the LHC across all $p_T$ regions. Consequently, this technique can pave the way for the precision studies of the CGC next-to-leading-order predictions by confronting them with a large amount of precise data.

DOI: 10.1103/PhysRevLett.128.202302

*Introduction.*—The gluon saturation phenomenon [1–6], predicted by the small-$x$ framework, which is also known as the color glass condensate (CGC) formalism, has been an intriguing forefront research topic. A lot of experimental and theoretical research efforts around the globe have been devoted to this cutting-edge research frontier. Besides, in the upcoming era of the electron-ion collider (EIC) [7–10], probing the emergent properties of ultradense gluon has become one of the key fundamental questions that the EIC sets out to address.

CGC is an effective formalism in quantum chromodynamics (QCD) which describes the novel nonlinear dynamics of low-momentum gluons inside a hadron. These low momentum gluon degrees of freedom are generally referred to as the small-$x$ gluons, with $x$ being the longitudinal momentum fraction. First, color sources such as large-$x$ quarks and gluons inside fast-moving hadrons emit a large number of small-$x$ gluons [11,12]. Usually, we introduce the saturation momentum $Q_s(x)$ at given $x$ to characterize the typical size of soft gluons. Because of the rise of the gluon density, $Q_s(x)$ increases at low $x$ so that the corresponding gluon size becomes smaller in the transverse space and more gluons can fit into a confined transverse region. This nonlinear dynamics can be captured by the Balitsky-Kovchegov and Jalilian-Marian–Iancu–McLerran–Weigert–Leonidov–Kovner (BK and JIMWLK) equation [13–18].

In high-energy collisions, small-$x$ gluon degrees of freedom are unlocked and measured in terms of final state hadrons. To search for the experimental evidence of gluon saturation among existing data [19–28] and prepare for the future EIC precision studies, it is important to develop next-to-leading order (NLO) computations in the CGC formalism and achieve an accurate description of data collected from various kinematic regions.

Among many different physical processes studied at RHIC and the LHC, the calculation and measurements of the single forward hadron production in proton-nucleus collisions (or deuteron-nucleus collisions at RHIC), $p(d) + A \to h(y, p_T) + X$, have attracted a great deal of attention [29–49]. In the forward region, the projectile proton (or deuteron) can be viewed as a relatively dilute object that probes the ultradense gluon fields in the nuclear target [30,36,37,50,51]. Experimentally, the evolution of the nuclear modification factor $R_{d\mathrm{Au}}$ [19,20] from midrapidity to forward-rapidity regions is considered the evidence [39,52–55] for the onset of gluon saturation. The measured $R_{d\mathrm{Au}}$ is computed from the hadron spectra in deuteron + gold collisions normalized by the spectra in $pp$ collisions times the number of binary collisions, and $R_{d\mathrm{Au}}$ in forward rapidity regions is found to be suppressed.

In terms of the perturbative expansion, the corresponding cross section can be schematically cast into

$$\frac{d\sigma}{dyd^2p_T} = \int x_p f_a(x_p) \otimes D_a(z) \otimes \mathcal{F}_a^{x_g}(k_\perp) \otimes \mathcal{H}^{(0)} + \frac{\alpha_s}{2\pi} \sum_{a,b=q,g} \int x f_a(x) \otimes D_b(z) \otimes \mathcal{F}_{ab}^{x_g} \otimes \mathcal{H}_{ab}^{(1)}, \tag{1}$$

where the first term stands for the leading order (LO) contribution first computed in Refs. [30,56] and the second term represents the NLO corrections derived from one-loop diagrams. In our framework, the full NLO contribution includes the contributions computed in Ref. [36,37] and the additional kinematic constraint corrections given in Ref. [45]. The kinematic variables are defined as follows, $x_p = (k_\perp/\sqrt{s})e^y$, $x_g = (k_\perp/\sqrt{s})e^{-y}$, $p_T = zk_\perp$ with $k_\perp$ and $z$ being the parton transverse momentum and the longitudinal momentum fraction of produced hadron with respect to its original parton, respectively.

The LO production in various channels and the contribution together with running coupling effects have been calculated extensively in Refs. [32,33,35,38,41,42,57–59], and part of the NLO contributions are studied in Refs. [34,56]. To obtain the full analytical expressions of the NLO corrections, one needs to evaluate all of the real and virtual one-loop diagrams and remove various types of divergences, as demonstrated in Refs. [36,37]. First, we subtract the so-called rapidity divergences and absorb them into the evolution of the dipole scattering amplitude associated with the dipole gluon distribution $\mathcal{F}^{x_g}(k_\perp)$. This procedure reproduces the well-known BK equation [13,14] and allows us to resum the small-$x$ large logarithms systematically. Second, one can gather all the residual collinear divergences and remove them through the redefinition of collinear parton distribution functions (PDFs) $xf(x)$ or/and fragmentation functions (FFs) $D(z)$. Eventually, the resulting finite NLO corrections, which are simplified in the large $N_c$ limit and denoted as $\mathcal{H}_{ab}^{(1)}$ in Eq. (1), can be numerically evaluated.

The direct evaluation of the complete NLO cross section yields a good agreement with experimental data [19,20] from RHIC for forward rapidity hadron production in the low-$p_T$ region. However, the NLO result drastically turns negative in the high $p_T$ region [40]. When the kinematic constraint corrections are included [45], the negative NLO cross-section issue can be slightly mitigated but not entirely resolved. In usual perturbative QCD calculations in the collinear factorization, similar issues occur as well for various processes. It indicates that large (and mostly negative) logarithms hidden in $\mathcal{H}_{ab}^{(1)}$ become important in the high $p_T$ region. In particular, in our case with the forward rapidity hadron production, the threshold logarithms cause the breakdown of the perturbative expansion, and they should be resummed in order to restore the predictive power of our calculation in the region of interest.

The quest for positivity in this NLO CGC calculation has sparked a lot of interest. Over the last seven years, there have been a lot of studies [43–49,60–65] dedicated to addressing the issue caused by the large negative NLO corrections. We believe that the threshold resummation is one of the feasible solutions to this issue, and the resummation technique developed in this work can also be useful in the study of other NLO calculations [66–75] in CGC. In addition, there have been some further theoretical efforts [76–79], which go beyond the eikonal approximation and compute the next-to-eikonal corrections for this process.

*Implementation of the threshold resummation.*—To tackle the issue of the large negative corrections at NLO, we need to analytically extend the applicability of the NLO CGC calculation from the low-$p_T$ region to the high-$p_T$ region, thus obtain reliable numerical predictions for measurements at both RHIC and the LHC, and therefore better understand the transition from the ultradense regime to the dilute regime. First, to illustrate the origin of the threshold logarithms in the NLO corrections, let us discuss the appearance of the large NLO corrections that cause the issue in the sufficiently forward rapidity region when $p_T \gg Q_s$ [40,45]. In fact, this indicates that the issue occurs when hard scatterings dominate in this region, where the corresponding events are approaching the kinematic threshold. Second, we identify and extract the large logarithms in the momentum space where the numerical computation of the NLO correction can be performed more efficiently. In the end, we introduce the resummation scheme, which allows us to take the higher-order large logarithms into account and restore the predictive power of the one-loop calculation for this process in the CGC framework.

To see this clearly and intuitively, let us recall the kinematics at NLO [36,37] and define the hadron longitudinal momentum fraction $\tau = (p_T/\sqrt{s})e^y$, which is equivalent to $\tau = x\xi z$ with $\xi$ being the remaining momentum fraction of a parton after emitting one gluon. In the forward rapidity region ($y > 0$), as the hadron $p_T$ increases, $\tau$ starts to approach 1. That is to say that we are approaching the threshold region where $x$, $z$, and $\xi$ are all forced to approach 1. In this case, the phase space for the real gluon emission is severely limited since there is not much longitudinal momentum left for the radiation near the threshold. In contrast, there is no constraint imposed on the virtual graphs. As a result, after canceling singularities between real and virtual graphs, large logarithms appear in the NLO corrections. These large threshold logarithms are the culprits that upset the convergence of the $\alpha_s$ expansion in our NLO calculation. Two formulations of the threshold resummation within the CGC framework have been

proposed earlier in Ref. [62] and Refs. [64,65], respectively. In this Letter, our study follows closely with the former approach.

Our strategy is described as follows. Initially, the NLO corrections [36,37] were derived in the coordinate space where the physical interpretation for gluon saturation is manifest. However, due to the oscillating behavior of the complex phase factor in the coordinate space expression, it is challenging to evaluate them numerically, especially in the high $p_T$ region. Therefore, we later transform the complete NLO cross sections, including the kinematic constraint corrections [45] into the momentum space, yielding much better numerical accuracy. In the coordinate space, we can identify two types of logarithms [62,80]

$$\text{single log}: \ln\frac{k_\perp^2}{\mu_r^2}, \quad \ln\frac{\mu^2}{\mu_r^2}; \quad \text{double log}: \ln^2\frac{k_\perp^2}{\mu_r^2}, \tag{2}$$

where $\mu_r \equiv c_0/r_\perp$ with $r_\perp$ being the dipole size and $c_0 = 2e^{-\gamma_E}$. After integrating over $r_\perp$ in the coordinate space, these logarithms coupled with plus functions generate large contributions in the threshold region when $k_\perp$ (or $p_T$) becomes much larger than typical value of $\mu_r$. Therefore, in the momentum space, we need to introduce an auxiliary semihard scale $\Lambda$, much larger than the QCD scale $\Lambda_{\rm QCD}$, to extract these large logarithms for the resummation purpose. The scale $\Lambda$ characterizes the typical transverse momentum scale carried by semihard gluons due to the Sudakov radiation and small-$x$ effect. In the momentum space, the single and double logarithmic terms can be correspondingly cast into [45,81,82]

$$\text{single log}: \ln\frac{k_\perp^2}{\Lambda^2} + I_1(\Lambda) \quad \text{and} \quad \ln\frac{\mu^2}{\Lambda^2} + I_1(\Lambda), \tag{3}$$

$$\text{double log}: \ln^2\frac{k_\perp^2}{\Lambda^2} + I_2(\Lambda), \tag{4}$$

where $I_{1,2}(\Lambda)$ represent the residual matching functions. At one-loop order, our results are independent of the choice of the auxiliary scale $\Lambda$. The essential steps of the derivations can be found in Supplemental Material [83].

Usually, in the collinear factorization, the threshold logarithms are resummed in terms of the resummation of the "plus" distributions in the Mellin moment space [84–87]. The technique employed in the CGC framework is slightly different since the relevant gluon distribution is transverse momentum dependent. The threshold logarithms in forward hadron productions can be cast into two parts: the soft and the collinear parts. The soft part such as single and double logs of $\ln(k_\perp^2/\Lambda^2)$, associated with the soft gluon emission, can be resummed by the Sudakov factor $S_{\rm Sud}(k_\perp, \Lambda)$. As to the collinear part ($\ln(\mu^2/\Lambda^2)$), there are two similar approaches to deal with the corresponding resummation. The first method is to develop a renormalization group equation [whose solution is $\Delta(\Lambda^2, \mu^2, \omega \equiv \ln 1/\xi)$] in the momentum space to analytically resum logarithms of $\ln(\mu^2/\Lambda^2)$ combined with the above soft part in the threshold limit with $\xi \to 1$. This scheme is akin to the method first developed in the pioneering study [88–91] for the deep-inelastic structure function using the soft-collinear effective theory.

Alternatively, since the above collinear logarithms are associated with the Dokshitzer-Gribov-Lipatov-Altarelli-Parisi (DGLAP) splitting functions, they can be resummed with the help of the DGLAP evolution of the PDFs and FFs by resetting the factorization scale [62] from $\mu$ to the auxiliary scale $\Lambda$ in the LO resummed terms and then the resummed formula reads

$$\sigma = \int xf_a(x,\Lambda) \otimes D_a(z,\Lambda) \otimes \mathcal{F}_a^{x_g}(k_\perp) \otimes \mathcal{H}^{(0)} \otimes e^{-S_{\rm Sud}} + \frac{\alpha_s}{2\pi}\int xf_a(x,\mu) \otimes D_b(z,\mu) \otimes \mathcal{F}_{ab}^{x_g} \otimes \mathcal{H}_{ab}^{(1)}(\mu,\Lambda). \tag{5}$$

In fact, this choice of the factorization scale $\mu$ for LO cross section is similar to the conventional practice of setting $\mu = \mu_b$ in the Collins-Soper-Sterman formalism [92]. These two resummation schemes are theoretically equivalent, and they yield similar numerical results. The resummation scheme is not unique, and one can certainly develop a similar scheme in the coordinate space as well.

Let us compare the resummed formulas as in Eq. (5) to the original NLO results in Eq. (1). Essentially, we take out the logarithmic term hidden in $\mathcal{H}_{ab}^{(1)}$ from Eq. (1), and extract the threshold logarithms which are resummed in Eq. (5). Then, the terms that are proportional to the residual matching functions $I_{1,2}(\Lambda)$ are put back into the new NLO coefficient $\mathcal{H}_{ab}^{(1)}(\mu,\Lambda)$. Initially, Eq. (1) only depends on the factorization scale $\mu$. After the implementation of the threshold resummation, Eq. (5) now depends on the choice of the factorization scale $\mu$ and the auxiliary scale $\Lambda$. Both scale dependences cancel to the one-loop order (NLO), and the residual scale dependences, which start from the two-loop order in this process, are due to the truncation of the perturbative expansions. Loosely speaking, the threshold-Sudakov resummation can effectively decrease the negative contributions at the one-loop order and therefore makes the resummed result positive.

In principle, the cross section would be independent of both $\mu$ and $\Lambda$ if all-order results were included. In practice, we can estimate the size of higher-order corrections by varying these two scales. Furthermore, to minimize the higher-order corrections, the "natural" choice of these two scales should be adopted. In the collinear part, the hard scale $Q$ ($\sim 2k_\perp$ when $k_\perp$ is sufficiently large) sets the scale for the factorization scale $\mu$. As to the semihard auxiliary scale $\Lambda$, the "natural" choice should be $\mu_r = c_0/r_\perp$, which

depends on the typical value of $r_\perp$ when $r_\perp$ is integrated over. Following Refs. [92–94], we use the saddle point approximation to locate the dominant region of the $r_\perp$ integral, thus estimate the physical value of $\Lambda$ via the running coupling prescription

$$\Lambda^2 \approx \max\left\{\Lambda^2_{\rm QCD}\left[\frac{(1-\xi)k_\perp^2}{\Lambda^2_{\rm QCD}}\right]^{\frac{C_R}{C_R+N_c\beta_0}}, Q_s^2\right\}, \tag{6}$$

where $\beta_0 = (11/12) - (n_f/6N_c)$. $C_R$ is the Casimir factor, which gives $C_F$ and $C_A$ for the quark and gluon channel, respectively. In the gluon channel, the saturation momentum $Q_s^2$ is increased by a factor of $N_c/C_F$ as compared to the quark channel. We set $\Lambda^2 = Q_s^2$ when the saturation effect is strong, while $(1-\xi)k_\perp^2 \sim (1-\tau)p_T^2$ becomes the dynamical scale near the threshold region [90,91].

*Numerical results.*—In the numerical evaluation, we use the NLO Martin-Stirling-Thorne-Watt (MSTW) PDFs [95] and NLO de Florian-Epele-Hernandez-Pinto-Sassot-Stratmann FFs [96] together with the one-loop running coupling. For the dipole gluon distribution $\mathcal{F}_a^{x_g}(k_\perp)$, we use the modified McLerran-Venugopalan model [4,5,97–100] with parameters given by the Set $h$ in Table I of Ref. [101] as the initial condition, solve the running-coupling BK equation numerically in the coordinate space [101–110], and then obtain the numerical inputs in the momentum space via Fourier transform. As shown in Ref. [41], the numerical results are sensitive to the above inputs especially the initial condition for $\mathcal{F}_a^{x_g}(k_\perp)$. To universally describe the data from RHIC and the LHC, it is important to choose proper initial conditions, include the NLO corrections, and implement the threshold resummation near the kinematic threshold.

As shown in Fig. 1, with the proper choices of the $\Lambda^2$ scales, the improved NLO CGC calculations with the implementation of the threshold resummation, which are labeled in red gridded bands, agree with the data collected at RHIC and the LHC in both low and high $p_T$ regions. Similar to Ref. [87], the edges of the various bands were computed by varying $\Lambda^2$ in the appropriate ranges and $\mu^2 = \alpha^2(\mu^2_{\rm min} + p_T^2)$ with $\alpha = 2 \sim 4$. To ensure that $\mu^2$ is not too small in the low $p_T$ region, a minimum value $\mu_{\rm min} = 2$ GeV is used. In the high $p_T$ region, the factorization scale is set by the hard scale $Q$, which is estimated to be at least twice the parton transverse momentum $k_T$. Therefore, the proper value of $\mu$ should be larger than $2p_T$ in this region.

Compared to the one-loop results marked in orange bands, the resummed results, which are depicted in red grids, are roughly unchanged in the low-$p_T$ region. In fact, when $\Lambda$ is set to the value around $\mu \sim k_\perp$, the resummation formulation naturally reduces to the one-loop result since the threshold logarithms become small in this limit. Meanwhile, the resummation significantly improves the stability of the NLO calculation for the high-$p_T$ spectrum

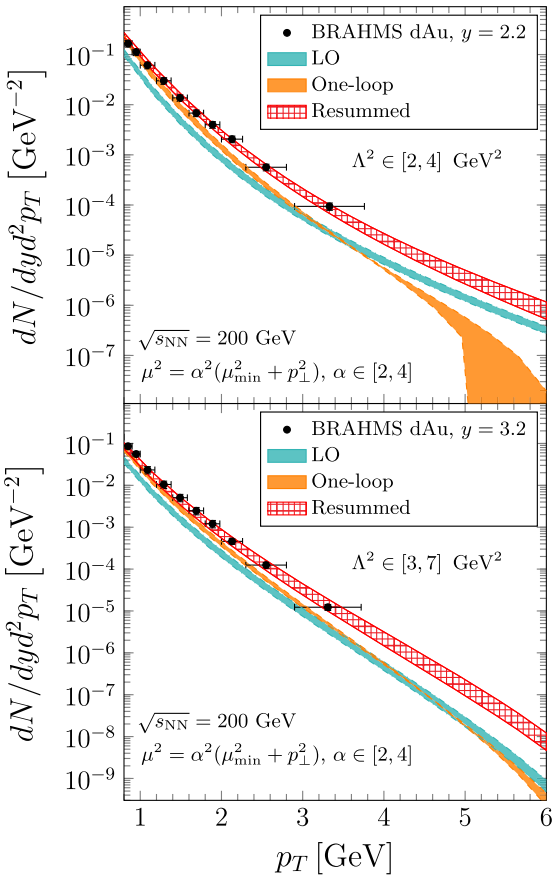


FIG. 1. Theoretical results computed in the CGC framework compared with the BRAHMS data [19]. Many additional plots are provided at the end of the Supplemental Material [83].

with the values of the auxiliary scale $\Lambda^2$ prescribed by Eq. (6).

In addition, we compare our calculation with the latest data measured by the LHCb Collaboration [28] in Fig. 2. In the forward rapidity regions, LHCb measured the prompt charged particle production in $pPb$ and $pp$ collisions at 5 TeV in five rapidity ranges around $y = 2.25$, 2.75, 3.25, 3.75, and 4.2. Within the same framework, we obtain a good agreement with the hadron spectra measured in both $pPb$ and $pp$ collisions for all rapidity windows. The impact of the resummation at the LHCb regime is less pronounced than that at RHIC since the kinematic range of this measurement is still far away from the threshold boundary.

Eventually, this allows us to calculate the nuclear modification factor, which is defined as

$$R_{pPb} = \frac{1}{A}\frac{d^2\sigma_{pPb}/dp_T dy}{d^2\sigma_{pp}/dp_T dy}. \tag{7}$$

The suppression of this factor $R_{pPb}$ reflects the onset of the small-$x$ evolution effect and the gluon saturation phenomenon. As we increase the rapidity or decrease the transverse

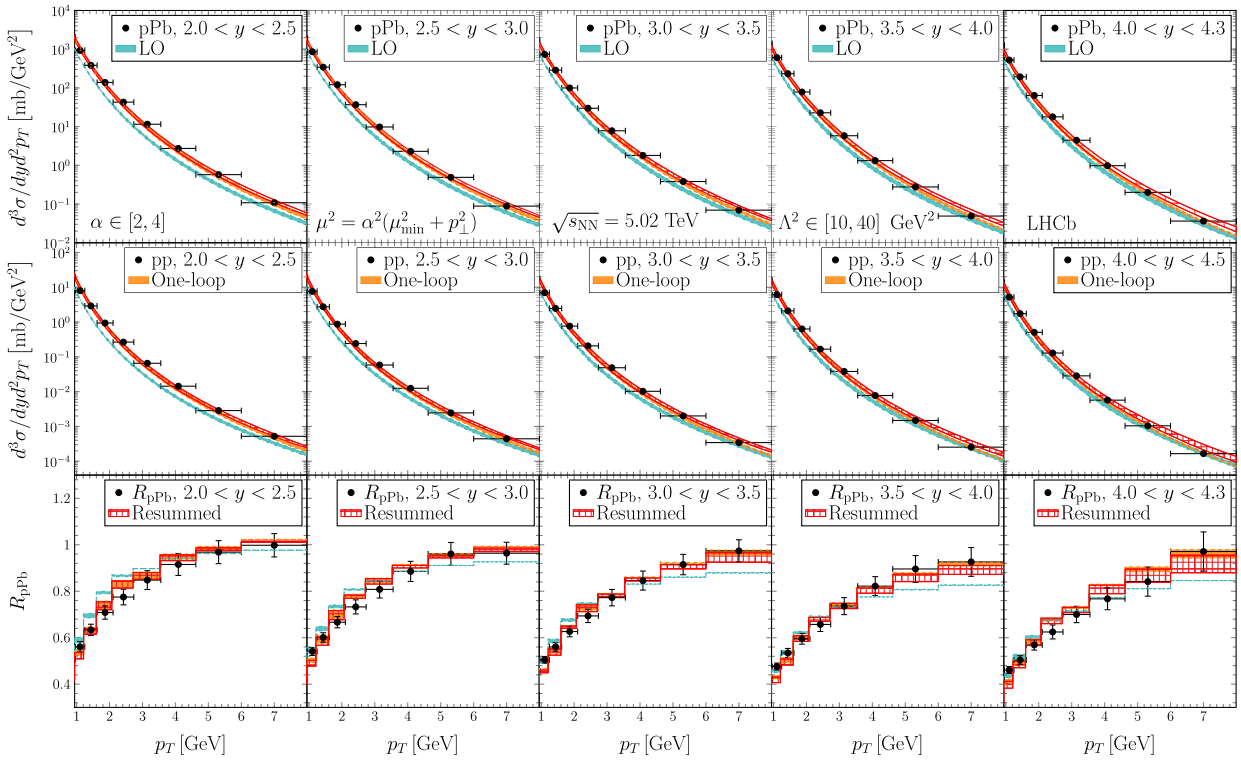


FIG. 2. Comparisons of the $pPb$, $pp$, and $R_{pPb}$ data [28] from LHCb with CGC calculations in five forward rapidity bins.

momentum, more suppression in $R_{pPb}$ as shown in Fig. 2 can be observed as the indication of strengthening of the small-$x$ evolution effect [52]. In the high $p_T$ region, $R_{pPb}$ approaches unity as the small-$x$ effect attenuates.

*Conclusion.*—By incorporating the threshold resummation in the CGC formalism, we extend the applicability regime of the CGC NLO calculation for forward hadron productions to the large transverse momentum region. Furthermore, the resummation allows us to reliably compute the hadron spectra and corresponding nuclear modification factor from low $p_T$ to high $p_T$ regions, and thus enables us to quantitatively understand the transition from the gluon saturation regime to the dilute regime. This study, which may serve as a benchmark example for other NLO CGC calculations, demonstrates that the NLO phenomenology is essential to test the CGC formalism and collect compelling evidence for the onset of gluon saturation. Last, the resummation formulation developed in this Letter can also shed light on other higher-order calculations in the CGC framework.

We thank Tuomas Lappi, Xiaohui Liu, Feng Yuan, and David Zaslavsky for useful inputs and discussions. This work is supported by the Natural Science Foundation of China (NSFC) under Grant No. 11575070 and by the university development fund of CUHK-Shenzhen under Grant No. UDF01001859.

*yu.shi@sdu.edu.cn
†leiwang@mails.ccnu.edu.cn
‡shuyi@sdu.edu.cn
§xiaobowen@cuhk.edu.cn

[1] L. V. Gribov, E. M. Levin, and M. G. Ryskin, Phys. Rep. **100**, 1 (1983).
[2] A. H. Mueller and J. w. Qiu, Nucl. Phys. **B268**, 427 (1986).
[3] A. H. Mueller, Nucl. Phys. **B335**, 115 (1990).
[4] L. D. McLerran and R. Venugopalan, Phys. Rev. D **49**, 2233 (1994).
[5] L. D. McLerran and R. Venugopalan, Phys. Rev. D **49**, 3352 (1994).
[6] F. Gelis, E. Iancu, J. Jalilian-Marian, and R. Venugopalan, Annu. Rev. Nucl. Part. Sci. **60**, 463 (2010).
[7] D. Boer, M. Diehl, R. Milner, R. Venugopalan, W. Vogelsang, D. Kaplan, H. Montgomery, S. Vigdor, A. Accardi, E. C. Aschenauer *et al.*, arXiv:1108.1713.
[8] A. Accardi, J. L. Albacete, M. Anselmino, N. Armesto, E. C. Aschenauer, A. Bacchetta, D. Boer, W. K. Brooks, T. Burton, N. B. Chang *et al.*, Eur. Phys. J. A **52**, 268 (2016).
[9] Y. Hatta, Y. V. Kovchegov, C. Marquet, A. Prokudin, E. Aschenauer, H. Avakian, A. Bacchetta, D. Boer, G. A. Chirilli, A. Dumitru *et al.*, *Probing Nucleons and Nuclei in High Energy Collisions* (World Scientific, Singapore, 2020).
[10] R. Abdul Khalek, A. Accardi, J. Adam, D. Adamiak, W. Akers, M. Albaladejo, A. Al-bataineh, M. G. Alexeev, F. Ameli, P. Antonioli *et al.*, arXiv:2103.05419.

[11] E. A. Kuraev, L. N. Lipatov, and V. S. Fadin, Sov. Phys. JETP **45**, 199 (1977).
[12] I. I. Balitsky and L. N. Lipatov, Sov. J. Nucl. Phys. **28**, 822 (1978).
[13] I. Balitsky, Nucl. Phys. **B463**, 99 (1996).
[14] Y. V. Kovchegov, Phys. Rev. D **60**, 034008 (1999).
[15] J. Jalilian-Marian, A. Kovner, A. Leonidov, and H. Weigert, Nucl. Phys. **B504**, 415 (1997).
[16] J. Jalilian-Marian, A. Kovner, A. Leonidov, and H. Weigert, Phys. Rev. D **59**, 014014 (1998).
[17] E. Iancu, A. Leonidov, and L. D. McLerran, Nucl. Phys. **A692**, 583 (2001).
[18] E. Ferreiro, E. Iancu, A. Leonidov, and L. McLerran, Nucl. Phys. **A703**, 489 (2002).
[19] I. Arsene *et al.* (BRAHMS Collaboration), Phys. Rev. Lett. **93**, 242303 (2004).
[20] J. Adams *et al.* (STAR Collaboration), Phys. Rev. Lett. **97**, 152302 (2006).
[21] E. Braidot (STAR Collaboration), Nucl. Phys. **A854**, 168 (2011).
[22] A. Adare *et al.* (PHENIX Collaboration), Phys. Rev. Lett. **107**, 172301 (2011).
[23] C. Hadjidakis (ALICE Collaboration), Nucl. Phys. B, Proc. Suppl. **214**, 80 (2011).
[24] B. Abelev *et al.* (ALICE Collaboration), Phys. Rev. Lett. **110**, 032301 (2013).
[25] B. Abelev *et al.* (ALICE Collaboration), Phys. Rev. Lett. **110**, 082302 (2013).
[26] G. Aad *et al.* (ATLAS Collaboration), Phys. Lett. B **763**, 313 (2016).
[27] R. Aaij *et al.* (LHCb Collaboration), J. High Energy Phys. 01 (2022) 166.
[28] R. Aaij *et al.* (LHCb Collaboration), Phys. Rev. Lett. **128**, 142004 (2022).
[29] Y. V. Kovchegov and A. H. Mueller, Nucl. Phys. **B529**, 451 (1998).
[30] A. Dumitru and J. Jalilian-Marian, Phys. Rev. Lett. **89**, 022301 (2002).
[31] A. Dumitru, A. Hayashigaki, and J. Jalilian-Marian, Nucl. Phys. **A770**, 57 (2006).
[32] J. L. Albacete and C. Marquet, Phys. Lett. B **687**, 174 (2010).
[33] E. Levin and A. H. Rezaeian, Phys. Rev. D **82**, 014022 (2010).
[34] T. Altinoluk and A. Kovner, Phys. Rev. D **83**, 105004 (2011).
[35] H. Fujii, K. Itakura, Y. Kitadono, and Y. Nara, J. Phys. G **38**, 124125 (2011).
[36] G. A. Chirilli, B. W. Xiao, and F. Yuan, Phys. Rev. Lett. **108**, 122301 (2012).
[37] G. A. Chirilli, B. W. Xiao, and F. Yuan, Phys. Rev. D **86**, 054005 (2012).
[38] J. L. Albacete, A. Dumitru, H. Fujii, and Y. Nara, Nucl. Phys. **A897**, 1 (2013).
[39] J. L. Albacete, N. Armesto, R. Baier, G. G. Barnafoldi, J. Barrette, S. De, W. T. Deng, A. Dumitru, K. Dusling, K. J. Eskola *et al.*, Int. J. Mod. Phys. E **22**, 1330007 (2013).
[40] A. M. Stasto, B. W. Xiao, and D. Zaslavsky, Phys. Rev. Lett. **112**, 012302 (2014).
[41] T. Lappi and H. Mäntysaari, Phys. Rev. D **88**, 114020 (2013).
[42] A. van Hameren, P. Kotko, K. Kutak, C. Marquet, and S. Sapeta, Phys. Rev. D **89**, 094014 (2014).
[43] A. M. Stašto, B. W. Xiao, F. Yuan, and D. Zaslavsky, Phys. Rev. D **90**, 014047 (2014).
[44] T. Altinoluk, N. Armesto, G. Beuf, A. Kovner, and M. Lublinsky, Phys. Rev. D **91**, 094016 (2015).
[45] K. Watanabe, B. W. Xiao, F. Yuan, and D. Zaslavsky, Phys. Rev. D **92**, 034026 (2015).
[46] A. M. Stasto and D. Zaslavsky, Int. J. Mod. Phys. A **31**, 1630039 (2016).
[47] E. Iancu, A. H. Mueller, and D. N. Triantafyllopoulos, J. High Energy Phys. 12 (2016) 041.
[48] B. Ducloué, T. Lappi, and Y. Zhu, Phys. Rev. D **93**, 114016 (2016).
[49] B. Ducloué, E. Iancu, T. Lappi, A. H. Mueller, G. Soyez, D. N. Triantafyllopoulos, and Y. Zhu, Phys. Rev. D **97**, 054020 (2018).
[50] F. Dominguez, B. W. Xiao, and F. Yuan, Phys. Rev. Lett. **106**, 022301 (2011).
[51] F. Dominguez, C. Marquet, B. W. Xiao, and F. Yuan, Phys. Rev. D **83**, 105005 (2011).
[52] D. Kharzeev, Y. V. Kovchegov, and K. Tuchin, Phys. Rev. D **68**, 094013 (2003).
[53] D. Kharzeev, Y. V. Kovchegov, and K. Tuchin, Phys. Lett. B **599**, 23 (2004).
[54] J. L. Albacete, N. Armesto, A. Kovner, C. A. Salgado, and U. A. Wiedemann, Phys. Rev. Lett. **92**, 082001 (2004).
[55] E. Iancu, K. Itakura, and D. N. Triantafyllopoulos, Nucl. Phys. **A742**, 182 (2004).
[56] A. Dumitru, A. Hayashigaki, and J. Jalilian-Marian, Nucl. Phys. **A765**, 464 (2006).
[57] J. P. Blaizot, F. Gelis, and R. Venugopalan, Nucl. Phys. **A743**, 13 (2004).
[58] J. P. Blaizot, F. Gelis, and R. Venugopalan, Nucl. Phys. **A743**, 57 (2004).
[59] M. Bury, H. Van Haevermaet, A. Van Hameren, P. Van Mechelen, K. Kutak, and M. Serino, Phys. Lett. B **780**, 185 (2018).
[60] Z. B. Kang, I. Vitev, and H. Xing, Phys. Rev. Lett. **113**, 062002 (2014).
[61] B. Ducloué, T. Lappi, and Y. Zhu, Phys. Rev. D **95**, 114007 (2017).
[62] B. W. Xiao and F. Yuan, Phys. Lett. B **788**, 261 (2019).
[63] H. Y. Liu, Y. Q. Ma, and K. T. Chao, Phys. Rev. D **100**, 071503(R) (2019).
[64] Z. B. Kang and X. Liu, arXiv:1910.10166.
[65] H. Y. Liu, Z. B. Kang, and X. Liu, Phys. Rev. D **102**, 051502(R) (2020).
[66] A. H. Mueller and S. Munier, Nucl. Phys. **A893**, 43 (2012).
[67] M. Hentschinski, J. D. M. Martínez, B. Murdaca, and A. Sabio Vera, Nucl. Phys. **B889**, 549 (2014).
[68] S. Benic, K. Fukushima, O. Garcia-Montero, and R. Venugopalan, J. High Energy Phys. 01 (2017) 115.
[69] R. Boussarie, A. V. Grabovsky, D. Y. Ivanov, L. Szymanowski, and S. Wallon, Phys. Rev. Lett. **119**, 072002 (2017).

[70] B. Ducloué, H. Hänninen, T. Lappi, and Y. Zhu, Phys. Rev. D **96**, 094017 (2017).
[71] K. Roy and R. Venugopalan, J. High Energy Phys. 05 (2018) 013.
[72] K. Roy and R. Venugopalan, Phys. Rev. D **101**, 071505(R) (2020).
[73] K. Roy and R. Venugopalan, Phys. Rev. D **101**, 034028 (2020).
[74] E. Iancu and Y. Mulian, J. High Energy Phys. 03 (2021) 005.
[75] P. Caucal, F. Salazar, and R. Venugopalan, J. High Energy Phys. 11 (2021) 222.
[76] T. Altinoluk, N. Armesto, G. Beuf, M. Martínez, and C. A. Salgado, J. High Energy Phys. 07 (2014) 068.
[77] T. Altinoluk, N. Armesto, G. Beuf, and A. Moscoso, J. High Energy Phys. 01 (2016) 114.
[78] G. A. Chirilli, J. High Energy Phys. 01 (2019) 118.
[79] T. Altinoluk, G. Beuf, A. Czajka, and A. Tymowska, Phys. Rev. D **104**, 014019 (2021).
[80] P. Sun and F. Yuan, Phys. Rev. D **88**, 114012 (2013).
[81] A. H. Mueller, B. W. Xiao, and F. Yuan, Phys. Rev. D **88**, 114010 (2013).
[82] P. Sun, C. P. Yuan, and F. Yuan, Phys. Rev. Lett. **113**, 232001 (2014).
[83] See Supplemental Material at http://link.aps.org/supplemental/10.1103/PhysRevLett.128.202302 for all the technical details and more numerical results.
[84] G. F. Sterman, Nucl. Phys. **B281**, 310 (1987).
[85] S. Catani and L. Trentadue, Nucl. Phys. **B327**, 323 (1989).
[86] S. Catani, M. L. Mangano, P. Nason, and L. Trentadue, Nucl. Phys. **B478**, 273 (1996).
[87] D. de Florian, W. Vogelsang, and F. Wagner, Phys. Rev. D **78**, 074025 (2008).
[88] S. W. Bosch, B. O. Lange, M. Neubert, and G. Paz, Nucl. Phys. **B699**, 335 (2004).
[89] T. Becher and M. Neubert, Phys. Lett. B **637**, 251 (2006).
[90] T. Becher and M. Neubert, Phys. Rev. Lett. **97**, 082001 (2006).
[91] T. Becher, M. Neubert, and B. D. Pecjak, J. High Energy Phys. 01 (2007) 076.
[92] J. C. Collins, D. E. Soper, and G. F. Sterman, Nucl. Phys. **B250**, 199 (1985).
[93] G. Parisi and R. Petronzio, Nucl. Phys. **B154**, 427 (1979).
[94] J. w. Qiu and X. f. Zhang, Phys. Rev. Lett. **86**, 2724 (2001).
[95] A. D. Martin, W. J. Stirling, R. S. Thorne, and G. Watt, Eur. Phys. J. C **63**, 189 (2009).
[96] D. de Florian, R. Sassot, M. Epele, R. J. Hernández-Pinto, and M. Stratmann, Phys. Rev. D **91**, 014035 (2015).
[97] K. J. Golec-Biernat and M. Wusthoff, Phys. Rev. D **59**, 014017 (1998).
[98] A. M. Stasto, K. J. Golec-Biernat, and J. Kwiecinski, Phys. Rev. Lett. **86**, 596 (2001).
[99] A. H. Mueller, Nucl. Phys. **B558**, 285 (1999).
[100] F. Gelis and A. Peshier, Nucl. Phys. **A697**, 879 (2002).
[101] J. L. Albacete, N. Armesto, J. G. Milhano, P. Quiroga-Arias, and C. A. Salgado, Eur. Phys. J. C **71**, 1705 (2011).
[102] K. J. Golec-Biernat, L. Motyka, and A. M. Stasto, Phys. Rev. D **65**, 074037 (2002).
[103] Y. V. Kovchegov and H. Weigert, Nucl. Phys. **A784**, 188 (2007).
[104] I. Balitsky, Phys. Rev. D **75**, 014001 (2007).
[105] E. Gardi, J. Kuokkanen, K. Rummukainen, and H. Weigert, Nucl. Phys. **A784**, 282 (2007).
[106] J. L. Albacete and Y. V. Kovchegov, Phys. Rev. D **75**, 125021 (2007).
[107] I. Balitsky and G. A. Chirilli, Phys. Rev. D **77**, 014019 (2008).
[108] J. Berger and A. M. Stasto, Phys. Rev. D **83**, 034015 (2011).
[109] H. Fujii and K. Watanabe, Nucl. Phys. **A915**, 1 (2013).
[110] E. Iancu, A. H. Mueller, D. N. Triantafyllopoulos, and S. Y. Wei, J. High Energy Phys. 07 (2021) 196.